Efficient electro-optic modulator for optical pumping of Na beams

J. F. Kelly and A. Gallagher[a)]

Joint Institute for Laboratory Astrophysics, University of Colorado and National Bureau of Standards, Boulder, Colorado 80309-0440

(Received 20 November 1986; accepted for publication 5 January 1987)

An electro-optic modulator using $LiTaO_3$ is described which yields 34% of the carrier intensity in each of the first-order sidebands with rf phase modulation frequencies $f_m \sim 1.0$ GHz and $\lesssim 1.0$ W input power. The modulator makes use of a lumped resonator with $Q \sim 200$ to obtain efficient production of the sidebands. It is shown that the device can be scaled for operation at ~ 2 GHz. Applications of this modulator include optical pumping of the lighter alkali atoms, *FM* sideband spectroscopy, and laser phase/frequency stabilization using rf modulation techniques.

INTRODUCTION

There are a number of applications, notably laser cooling techniques, where it is useful to prepare a beam of spin-polarized alkali atoms in the highest $F,|M|$ state of the ground manifold of hyperfine states.[1,2] Preparation of a beam of such atoms, to produce a "two-level" system, typically requires two laser frequencies to empty out the lower F,M states, which are initially populated and further repopulated by leakage due to imperfect circular polarization and other effects.[2,3] Past techniques employed either two separate cw lasers[4] or one standing wave laser cavity operated simultaneously at two mode frequencies to pump both sets of F levels. The same goal has been achieved by rf phase modulating an electro-optic (EO) crystal to obtain first-order sidebands separated by the appropriate hyperfine splitting.[3]

We report here an analogous technique for optically pumping a beam of Na into the $F,|M| = 2,2$ levels. In this technique we modulate at *half* the hfs frequency and use the first-order sidebands only. [By modulating an EO crystal at $\omega_m = \text{hfs}/2$ with sufficient rf power, one effectively obtains the two necessary cw frequencies with power $I_{\pm}^{\max}(\omega_0 \pm \omega_m) \approx 0.34\, I_0$ using one actively stabilized laser with power I_0.] The construction of a lumped EO resonator of moderate $Q(\sim 200)$, which can produce the maximum first-order sidebands with modest rf powers ($\lesssim 1$ W) is described. For our applications a modulation frequency of ~ 886 MHz is required, but we show that the device could be scaled to $f_m \sim 2$ GHz.

The principles of lumped and traveling wave EO modulators are well known[5] so we shall give only a first-order discussion of the principles in Sec. I. No attempt is made to analyze the EM fields of our device since experience has shown that the resonant frequency is sensitive to the geometry of rf coupling and parasitic reactances of the mounting/shielding box and feed-in cable. A more complete analysis of a similar resonant cavity modulator is given in Ref. 6. Since it is possible to tune the cavity by minor geometry adjustments, exacting construction and design principles are not needed. We believe this design has some practical advantages over previously reported designs because it is easy to construct and operate and less expensive in terms of the rf technology. The cavity is based on a split-ring resonator design used successfully in magnetic resonance work.[7] The layout of the resonator and inductive coupling used to excite the cavity are shown in Fig. 1.

The device we describe uses $LiTaO_3$ as the modulating medium. A prototype was also successfully built with $LiNbO_3$; however, it suffered photorefractive damage with light levels $\gtrsim 20$ mW/mm^2. The damage was reversible by heating the crystal above ~ 170 °C. The $LiTaO_3$ crystal shows no evident optical damage with extended use at light levels $\gtrsim 150$ mW/mm^2.

I. PRINCIPLES OF APPLICATION

The technique of generating rf sidebands on a laser field is based on the equivalence of phase modulation and frequency modulation given by[8]

$$E(t) = E_0 \sin(\omega_0 t + \eta \sin \omega_m t)$$

$$= E_0 \sum_{n=-\infty}^{\infty} J_n(\eta) \sin(\omega_0 + n\omega_m)t\,. \qquad (1)$$

Applying a sinusoidal change of phase $\eta \sin \omega_m t$ at modulation frequency ω_m on a pure sinusoidal input field yields an output field consisting of sidebands with amplitudes equal to the nth-order Bessel functions $J_n(\eta)$. For the case of light linearly polarized along the ith direction of an EO crystal, the modulation index η_{ij} is calculated from the linear electro-optical coefficients r_{ij} by the relation[8]

$$\eta_{ij} = \pi L n_i^3 r_{ij} E_j / \lambda_0\,. \qquad (2)$$

Here L is the length of the crystal, n_i is the index of refraction for the ith direction of light polarization, E_j is the applied electric field of modulation along the jth axis of the crystal, and λ_0 is the vacuum wavelength of the light field. Maximum first-order sidebands occur when $\eta \approx 1.84$ which yield $J_1^2(1.84) \approx 0.34$, $J_0^2(1.84) \approx 0.100$, and $J_2^2(1.84) \approx 0.100$. It is also possible to generate a sizable second-order sideband, which may be advantageous for some applications. One could obtain two fairly strong laser sources separated by several multiples (3–4) of the modulation frequency.

An estimate of the rf power needed to sustain this modu-

 0034-6748/87/040563-04$01.30

lation in $LiTaO_3$ and $LiNbO_3$ can be derived from the data given in Table I.[10] For comparison, the maximum first-order modulation η_{33} in $LiTaO_3$ is produced by applying a 43-V peak rf field across a 1-mm-sq bar with 25 mm length. A traveling wave resonator made from this crystal (with ~50-Ω impedance) must transmit about 16 W of rf power to obtain this modulation index. A lumped resonator with $Q \approx 100$ can sustain the same modulation index using < 1 W of rf to compensate for dielectric and skin losses in the cavity. For a practical comparison, our 3 (x axis) × 3 (z axis) × 25 (y axis) mm^3 $LiTaO_3$ crystal used ~1.5-W rf power while the traveling wave resonator of Ref. 3, with dimensions $0.6 \times 0.5 \times 25$ mm^3, used ~4–6 W of rf power to achieve the same index of modulation. This smaller crystal should yield nearly the same f_0 in our modulator and require $\ll 1$ W, but breakage is a serious concern and it was not tried. Longer crystals will use less rf power, but will have reduced bandwidth due to phase-velocity mismatch.[6]

A first-order analysis of the cavity shown in Fig. 1 assumes the resonator can be treated as a lumped $\mathscr{L}_{RC}$ tank circuit. This assumption seems reasonable since the high dc dielectric constant of $LiTaO_3$ ($\epsilon/\epsilon_0 \approx 43$) should concentrate the electric field lines within the gap filled by the EO crystal. If this is true then the gap can be treated as an ideal capacitor with lumped capacitance $\epsilon \omega L/d$. Here ϵ is the dielectric constant of the crystal at the modulation frequency ω_m. It follows, also, that the circulating current distribution along the inside cylinder wall is uniform, so the lumped inductance of the loop (with $L > r$) is nearly that given by an ideal cylindrical current sheet $\mu_0 \pi r^2/L$. This approximation is expected to hold when the gap is small compared to the loop circumference, i.e., $d \ll 2\pi r$. The resonant frequency of this series $\mathscr{L}C$ circuit is thus given as

$$f_0 = \frac{1}{2\pi}(\mathscr{L}C)^{-1/2} = \frac{1}{2\pi}\left(\frac{c}{r}\right)\left(\frac{d}{\pi \omega K}\right)^{1/2}, \qquad (3)$$

where $K = \epsilon(\omega_m)/\epsilon_0$ and c is the speed of light. It is noted that the operating frequency is independent of crystal length L. For the case of a $LiTaO_3$ crystal with $W/d = 1$ and modulated along the z axis, a resonant frequency of 860 MHz, appropriate for Na optical pumping, is obtained with $r \sim 0.49$ cm. The dc value of K is assumed. (Its value at 1 GHz is unknown and may be a substantial cause of error in calculating f_0.)

Power is coupled into the resonator by mutual inductance with a single-loop drive coil (Fig. 1). The effect this induction coil has on the resonant frequency of the modulator cavity has been ignored in Eq. (3) since the circuit is operated in the limit of low coupling coefficient κ between drive coil and resonator. Maximum rf power transfer occurs when $\kappa Q \sim 1$ so the limit of weak coupling can be achieved if the Q of the cavity is large. We have observed that the transfer of power for the circuit shown in Fig. 1 is large enough to store the necessary rf energy without much effort given to matching the circuit to the rf source impedance. One could use swept frequency reflection measurements to match the circuit and source for more critical applications.

TABLE I. Physical properties of $LiTaO_3$ and $LiNbO_3$ taken from Ref. 9.

	ϵ_3(dc)[a]	n_3[b]	r_{33}[c]	tan δ_l[d]
$LiTaO_3$	0.38	2.188	30.3	5×10^{-4}
$LiNbO_3$	0.25	2.217	30.8	N.A.

[a] in 10^{-9} f/m.
[b] at 0.60 μm.
[c] in 10^{-12} m/V at 0.633 μm and $f_m \sim 75$ MHz.
[d] for z axis at 1 GHz and 25 °C.

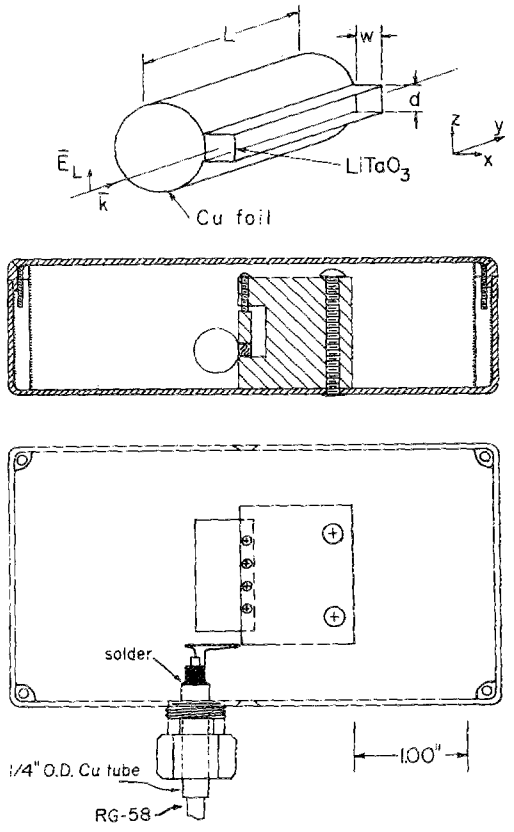

FIG. 1. Schematic of Cu foil resonator and scale drawing of operational modulator for 860 MHz. See text for details.

An estimate of the Q value of this circuit is difficult to make because it depends on several fabrication variables. The three notable loss mechanisms are (a) skin resistance which depends on the surface preparation of the metal loop; (b) dielectric loss in the EO crystal; and (c) rf losses to the surrounding structure which supports the cavity. We do not attempt to specify the last effect except to note that we were careful to construct the supporting structure from low dielectric loss plastics. The dielectric loss of the crystal is calculated given the loss tangent tan δ_l. The total power $P^{(b)}$ dissipated in the crystal is[11]

$$P^{(b)} = (V^2/2)G.$$

Here G is the effective parallel conductance of the crystal, given by

$$G = \omega_m C \tan \delta_l .$$

The $Q^{(b)}$ of the circuit with only this loss is

$$Q^{(b)} \equiv 2\pi \frac{\text{Energy stored per cycle}}{\text{Energy lost per cycle}} = \frac{\pi \omega_m C V^2}{P^{(b)}} = 2\pi/\tan \delta_l . \qquad (4)$$

Assuming $\tan\delta_l \approx 5\times10^{-4}$ at 1 GHz for $LiTaO_3$ yields $Q > 10^4$. The Q value which would result from the finite conductance σ of the metal foil is calculated similarly and gives[7]

$$Q = r/\delta ,$$

where δ is the skin depth and r the radius of the coil. The former quantity is given by

$$\delta = \left(\frac{2}{\mu_0\omega_m\sigma}\right)^{1/2} .$$

Quoting Ref. 7, at 1 GHz the conductivity of Cu, 0.5×10^6 $(\Omega\ \text{cm})^{-1}$, results in a skin depth δ of 2.4 μm. Thus, a highly polished Cu loop (scratch depth $< 1\ \mu$m) should result in $Q^{(a)} \gtrsim 10^3$. Generally, our resonators had an order of magnitude smaller $Q(\sim 200)$ as measured by

$$Q = \omega_0/\Delta\omega(\text{FWHM}) .$$

II. CONSTRUCTION AND OPERATION OF MODULATOR

The $LiTaO_3$ crystal used in our work is a $3\times3\times25\ \text{mm}^3$ bar with the x and z axes along the shorter dimensions. The y faces are broadband AR coated with a multilayer coating. A more cost-effective AR coating might be a single $\lambda/4$ layer of MgF_2 since $n(MgF_2) \approx [n(LiTaO_3)]^{1/2}$.[12] A final caveat concerning AR coatings: A coating vendor should be made aware that $LiTaO_3$ has a very large pyroelectric coefficient; large temperature changes in time will produce large electric fields along the crystal which may result in discharging.[12]

The resonator shown in Fig. 1 was formed from 0.005-in. Cu foil. Two tabs ($3\times25\ \text{mm}^2$) were initially bent at right angles to form a shallow C channel. A layer of indium was soldered to each of the tab faces to improve electrical contact of the foil and crystal. The cylinder of the resonator was then formed around a $\frac{13}{32}$-in. hardened and polished steel pin gauge taking care not to scratch the Cu surface unduly.

The surfaces of the indium coatings were then "dressed up" as follows: A hard, polished spacer (a sapphire window works very well) of the requisite thickness was inserted between the tabs (the indium is facing inside the gap) and this assembly was squeezed in a machinists' vise with well-polished jaws. The soft indium flowed to form a mirror finish on each tab; the excess flow over the edges was trimmed off. Several interations of this process can be performed to obtain a very thin layer of indium ($\lesssim 0.0005$ in.).

The assembly of crystal and foil resonator was clamped together with a low dielectric loss plastic vise as shown in Fig. 1, and mounted in an Al shield box with 2 $\frac{1}{4}$-in.-W$\times$4 $\frac{1}{4}$-in.-L$\times$1 $\frac{1}{8}$-in.-H. The primary induction coil consisted of a simple loop termination of the inner wire of RG-58 coax cable to its sheath; the diameter of the loop was nearly the same as the resonator coil. Before adding this loop, a $\frac{1}{4}$-in.-o.d. Cu tube sleeve was fitted over the outer plastic sheath of the RG-58 cable and this was passed through a compression fitting mounted to the Al box. The feed-in position can be fixed securely by finger-tightening this fitting. In this way, one can smoothly adjust the mutual inductance between the drive and resonator loops to obtain the best coupling.

The resonant frequency f_0 of the EO cavity and drive coil can be measured with swept frequency reflection measurements, however, we opted to measure the modulator f_0 by placing a second loop antenna near the cavity to pick up the resonance condition. The weak coupling limit will apply to the pick-up coil also, so the measured f_0 is only slightly different than the actual frequency of operation. [Figure 2 shows the additional port on the power splitter for measuring reflected power; this is a suggested improvement (Ref. 12) for ease of implementation.] With the dimensions noted, we measured the initial resonant frequency to be near 860 MHz. This compares well with a calculated $f_0 \sim 806$ MHz using Eq. (2) with $K = K_{dc} \approx 43$. However, the match is probably coincidental, as we show later.

Figure 2 shows the operational setup of our device. The sideband intensity is measured directly with a 2-GHz optical spectrum analyzer. The voltage controlled oscillator frequency is monitored with a 1-GHz counter while tuning for maximum optical pumping for Na (≈ 886 MHz). The first-

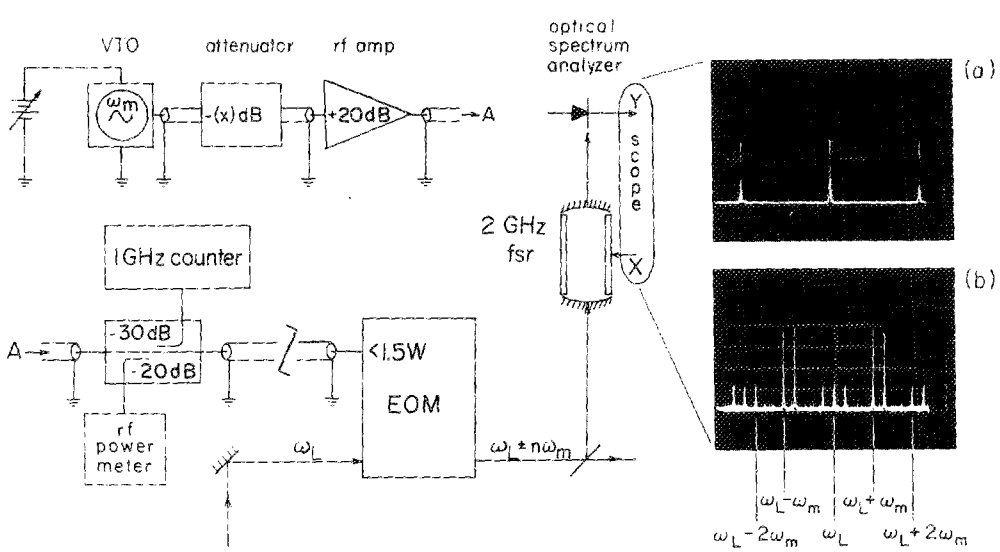

FIG. 2. Schematic of modulator technology. VTO = varactor tuned oscillator. The oscillograph trace shown in (a) is for the case of no modulation. The spectrum orders are separated by 2 GHz. Trace (b) shows the case with modulation index $\eta \sim 1.8$. The following components, which provide a low-cost solution for the rf technology, were used: VTO (0.6–1.0 GHz with 10-mW output power) Avantek VTO-8060, rf amplifier (10–10 000 MHz, $\gtrsim 1.0$ W output) Mini-Circuits ZHL-2-8, frequency counter (50 Hz–1.0 GHz) Digimax Instruments Corp. (The names of the various instruments have been specified for technical completeness and should not be considered an endorsement of particular products.)

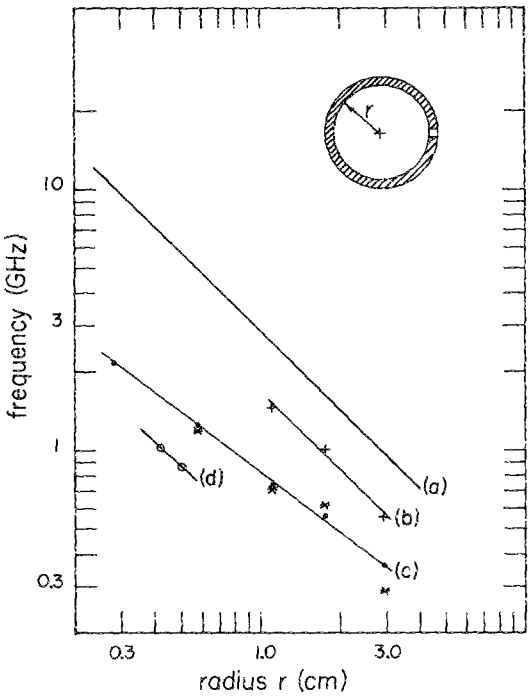

FIG. 3. Frequency response of split ring resonator: (a) response based on Eq. (3) with $w = 0.112 \times d = 0.127$ cm^2 and airspaced ($K = 1$); (b) measured response of same with 25-mm L Cu ring and airspace; (c) measured response of same with $LiTaO_3$ crystal added; (d) measured response of operational foil resonator based on Fig. 1 with $r = 0.516$ cm.

order sideband amplitudes are then maximized by adjusting the attenuation between the oscillator and amplifier stages.

One drawback of this resonator design is its temperature-dependent resonant frequency. The resonator takes an hour to equilibrate to a higher operating temperature (~ 50 °C) as it dissipates energy. This heating alters the performance of the device by shifting the resonant frequency downward. The Q of the cavity is reduced also, since $\tan \delta_l$ increases with temperature.[10] (It also probably alters η because ϵ and r_{ij} are temperature-dependent parameters, but data are not available concerning their temperature dependence.)

This is not a critical problem in our experiment since we allow the modulator to reach equilibrium; any small changes after this are not important since the intensity of the sidebands is sufficient to achieve optical saturation. For this purpose the modulator's initial resonant frequency is readjusted to a higher f_0 which then settles to the desired operating frequency. f_0 can also be adjusted by deforming the cylindrical coil of the resonator to an elliptical cross section. The largest inductance, hence lowest f_0, results when the coil is circular since this form encloses the greatest area with the shortest boundary. (The ratio of magnetic flux to current density is maximal.) A consequence of this procedure is the reduction of Q, but this is tolerable in our applications since $Q \sim 200$ at 860 MHz was reduced to $Q \sim 156$ at 890 MHz. External cooling/temperature stabilization should eliminate this problem for more critical applications.

It should be practical to scale this lumped EO modulator to higher frequencies, subject to phase-matching considerations as the crystal length becomes a significant fraction of the rf wavelength.[6] In order to test the scaling properties of this device, a number of split-ring resonators were fabricated from OFHC copper as shown in the inset of Fig. 3. A crystal with dimensions 1.1 (x axis) $\times$ 1.3 (z axis) $\times$ 25 (y axis) mm^3 was used in this resonator design. The resonant frequencies of these cavities, shown in Fig. 3, were obtained using the second technique of frequency measurement discussed above. The Q's of these cavities, measured by $\omega_0/\Delta\omega$(FWHM), were ~ 100. These frequency measurements were performed with the cavities sitting ~ 7.5 cm above a metal plane on a dielectric block, but otherwise unshielded.

The difference between these results and the operational device are due to many factors such as the linkage geometry of the coils and external reactances. Placement of external metal objects within 0.5 m of an unshielded cavity shifted f_0 down ~ 3–5 MHz, which implies an rf shielding box will pose sizable perturbations. In lieu of this, Eq. (3) should only be used as a crude reference. The results of Fig. 3 also imply K at 1 GHz is significantly smaller than quoted values of $K_{dc} \approx 43$. A more precise evaluation of K and r_{33} (and their temperature dependence) should be performed for frequencies $\gtrsim 1$ GHz.

Nevertheless, the results of Fig. 3 imply that these devices can produce efficient rf frequency modulation in the range of 0.3–2.2 GHz. The efficiency of these devices makes them useful for applications requiring a large modulation index η at a fixed frequency. Two such applications are laser phase and frequency stabilization techniques requiring rf phase modulation,[13] and frequency-modulation spectroscopy.[14]

This work has been supported in part by the Fundamental Interactions Branch of the Department of Energy. The authors thank J. Hall for many fruitful suggestions and equipment loans in the course of developing this modulator, and his valuable criticisms of this manuscript. We also thank D. Z. Anderson for loaning us the $LiTaO_3$ crystal used in this work.

[a] Staff member, Quantum Physics Division, National Bureau of Standards.

[1] D. E. Pritchard, E. L. Raab, V. Bagnato, C. E. Wieman, and R. N. Watts, Phys. Rev. Lett. **57**, 310 (1986).
[2] R. Blatt, W. Ertmer, and J. L. Hall, Prog. Quantum Electron. **8**, 237 (1984).
[3] W. Ertmer, R. Blatt, J. L. Hall, and M. Zhu, Phys. Rev. Lett. **54**, 996 (1985).
[4] S. Chu, L. Hollberg, J. E. Bjorkholm, A. Cable, and A. Ashkin, Phys. Rev. Lett. **55**, 48 (1985), and references therein.
[5] See, e.g., I. P. Kaminow, *An Introduction to Electrooptic Devices* (Academic, New York, 1974), and references therein.
[6] T. F. Gallagher, N. H. Tran, and J. P. Watjen, Appl. Opt. **25**, 510 (1986).
[7] W. N. Hardy and L. A. Whitehead, Rev. Sci. Instrum. **52**, 213 (1981).
[8] See, e.g., I. P. Kaminow, *An Introduction to Electrooptic Devices* (Academic, New York, 1974), p. 213.
[9] See, e.g., I. P. Kaminow, *An Introduction to Electrooptic Devices* (Academic, New York, 1974), p. 167.
[10] Data supplied by Crystal Technology, 1035 E. Meadow Circle, Palo Alto, CA 94303.
[11] See, e.g., I. P. Kaminow, *An Introduction to Electrooptic Devices* (Academic, New York, 1974), p. 84.
[12] J. L. Hall, Joint Institute for Laboratory Astrophysics, Boulder, CO 80309-0440 (private communication).
[13] R. W. P. Drever, J. L. Hall, F. V. Kowalski, J. Hough, G. M. Ford, A. J. Munley, and H. Ward, Appl. Phys. B **31**, 97 (1983).
[14] J. L. Hall, L. Hollberg, T. Baer, and H. G. Robinson, Appl. Phys. Lett. **39**, 680 (1981), and references therein.